# Event-by-Event Analysis of Proton-Induced Nuclear Multifragmentation: Determination of the Phase Transition Universality Class in a System with Extreme Finite-Size Constraints

M. Kleine Berkenbusch, W. Bauer,* K. Dillman, and S. Pratt

*National Superconducting Cyclotron Laboratory and Department of Physics and Astronomy, Michigan State University, East Lansing, Michigan 48824-1116*

L. Beaulieu,† K. Kwiatkowski,‡ T. Lefort,§ W.-c. Hsi,‖ and V. E. Viola

*Department of Chemistry and IUCF, Indiana University, Bloomington, Indiana 47405*

S. J. Yennello

*Department of Chemistry and Cyclotron Laboratory, Texas A&M University, College Station, Texas 77843*

R. G. Korteling

*Department of Chemistry, Simon Fraser University, Burnaby, British Columbia, Canada V4A 1S6*

H. Breuer

*Department of Physics, University of Maryland, College Park, Maryland 20742*

A percolation model of nuclear fragmentation is used to interpret 10.2 GeV/$c$ $p$ + $^{197}$Au multifragmentation data. Emphasis is put on finding signatures of a continuous nuclear matter phase transition in finite nuclear systems. Based on model calculations, corrections accounting for physical constraints of the fragment detection and sequential decay processes are derived. Strong circumstantial evidence for a continuous phase transition is found, and the values of two critical exponents, $\sigma = 0.5 \pm 0.1$ and $\tau = 2.35 \pm 0.05$, are extracted from the data. A critical temperature of $T_c = 8.3 \pm 0.2$ MeV is found.

    

Reactions in which excited nuclei break up into intermediate size fragments, nuclear multifragmentation reactions, are believed to be associated with a liquid-gas-type phase transition in nuclear matter. However, so far no unambiguous proof for this transition has been found in experimental data. This is due to, primarily, the extreme finite-size effect involved in systems of only on the order of $10^2$ constituents, the impossibility to fix a system at points in the phase diagram and study it there, as well as the complication due to sequential decays of the fragments produced in their excited state.

In this Letter we report results of an analysis of data on proton-induced fragmentation reactions of a $^{197}$Au target at incident energies of 10.2 GeV/$c$. These data were collected by the ISiS collaboration [1] in experiments at the Brookhaven National Laboratory AGS accelerator facility. A comparison with percolation-theory-based models is conducted. This comparison enables us to pay particular attention to detector efficiency effects, finite-size effects, as well as to the role played by sequential decay processes. With these corrections applied, an event-by-event scaling analysis is performed in order to derive values for the critical exponents $\sigma$ and $\tau$ and the critical temperature $T_c$ of the phase transition.

The ISiS Collaboration has produced one of the most complete experimental multifragmentation data sets with very high statistics. These data have also been interpreted in the framework of other phase transition models, in particular the SMM, EES, and SIMON models [2], usually associated with a liquid-gas-type phase transition. However, within the models the order of the phase transition depends on certain model parameters, as well as on the size of the system; see, for example, Ref. [3]. The percolation approach provides an effective alternative way for determining the order of the phase transition and the influence of finite-size effects.

The percolation model of nuclear multifragmentation used in our analysis has been introduced originally by Bauer *et al.* [4] and used by many groups [5]. It utilizes a representation of the target nucleus by sites of a simple cubic lattice ($\mathbf{Z}^3$) in an approximately spherical shape, with nearest-neighbor bonds representing the (short-ranged) strong force between the nucleons. These bonds are broken statistically independently with a probability $p_b$. Clusters of connected sites are counted and interpreted as fragments.

Multifragmentation reactions can be thought of as three-step processes. In the first step excitation energy is deposited in the target nucleus and preequilibrium particles are emitted. In the second step, the thermalized source breaks up into intermediate mass fragments. In the final step, the excited prefragments decay via standard sequential decay channels into the fragments that can be observed by the detector.

       

Step one, energy deposition: The percolation model needs a bond breaking probability $p_b$ as input. $p_b$ can be determined from the energy deposited in the system via

$$p_b(E^*) = 1 - \frac{2}{\sqrt{\pi}} \Gamma\left(\frac{3}{2}, 0, \frac{B}{T(E^*)}\right), \qquad (1)$$

where $\Gamma(x, z_0, z_1)$ is the generalized incomplete gamma function, $B$ is the binding energy per nucleon in the source, $T$ is the temperature of the source, and $E^*$ is the excitation energy per nucleon of the source [6]. It is assumed that the relation between the excitation energy $E^*$ of the fragmenting source and the temperature is given by $E^* = aT^2$ with $a = A_0/13$ (corresponding to the high temperature limit of a degenerate Fermi gas model; $A_0$ is the mass number of the residue nucleus; compare also [7]). Here we utilize the energy deposition and source size information as determined from the experimental data [1]. It can be argued that $a = A_0/8$ should be used for low excitation energies, where surface effects are dominant. However, close to the critical point surface effects disappear, and this motivates our choice of $a = A_0/13$. One should keep in mind, however, that this choice will have some (minor) consequences for the exact value of the critical value of the control parameter of the percolation model.

Step two, percolation: For the size of the lattice, we use the charge of the nucleus after emission of preequilibrium particles. Alternatively, one could also use the mass of the source. For the theory, this provides no difficulties whatsoever. However, in the experiment mostly the charges of the particles are detected. Thus it is natural to use the charge as the relevant quantity in our calculations. The assumption that the source has an approximately spherical shape after the emission of preequilibrium particles is supported by nuclear transport theory calculations in the BUU model [8]. After setting up the source on the lattice, the bonds are broken with the probability $p_b$ and the cluster structure is analyzed.

Step three, sequential decay: For this, we use a computer code we recently developed to investigate radioactive isotope yields in RIB facilities [9]. Eight decay modes were considered: proton, neutron, deuteron, dineutron, diproton, $t$, $^3$He, and $\alpha$. The decay weights were chosen according to Weisskopf arguments. For nuclei up to nitrogen experimentally measured values were used for the excited states. Decays were calculated for all levels in all nuclei. For the decay of each level, the decay rate was calculated into every possible level energetically accessible through the decay modes listed previously. The weight associated with the decaying nucleus was then apportioned into all the states in proportion to the rates for the decay into such states. The weights were also simultaneously added into the ground states of the nuclei representing the decay modes. Thus, the decaying process exactly preserved the initial $N$ and $Z$ of the original source system.

While the ISiS data set contains essentially complete events, it is still subject to the usual problems associated with multiparticle detector systems of subatomic particles, such as energy cuts, gaps between the active areas of the detector elements, loss of charge and mass resolution for heavier fragments, and fragments that escape detecting by being stopped in the target or traveling down the beam pipe. For the quantitative study we attempt here, these effects cannot be neglected. We have thus created extensive filter software to simulate detector acceptance effect.

Figure 1 shows the comparison of our calculations with the experimental data. The data points with the (very small) error bars represent the results of the experimental charge yields. The discontinuity at charge $Z = 17$ is due to the fact that only charges up to that value could be resolved elementally by the detector and the assumption that all missing mass is contained in a single residue (corrected for prompt particle emission during the fast cascade stage of the reaction). The dotted histogram is the result of our model calculations, as described in the previous section, without applying the filter. Filtering of our model calculations through the detector acceptance filter yields the thick histogram. It is in essentially perfect agreement with the data. The discrepancy between the two histograms thus gives us a good understanding of the degree to which the raw experimental data are affected by detector acceptance effects. One can also investigate more exclusive observables, such as the vanishing of the largest cluster as a function of the multiplicity, or the second moment as a function of the multiplicity. For the percolation model, these comparisons were published previously for other, but similar, data sets [10,11]. Here we obtain a similar degree of agreement. These comparisons, as well as a comparison
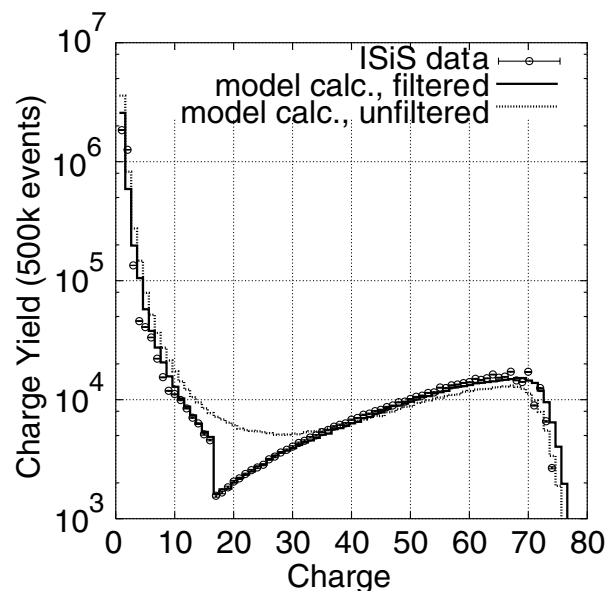


FIG. 1. Inclusive charge yield spectra for the reaction $p + $ Au at 10.2 GeV. The round plot symbols represent the ISiS dat. The dotted histogram is the result of the corresponding percolation model calculation. The thick histogram represents the output of the calculation, filtered through the detector acceptance corrections.

of a charge of the largest cluster for different multiplicity bins, have been performed [12] and will be published in a forthcoming paper.

From analytical solutions and numerical results on very large lattices, it can be inferred that in percolation theory, for the control parameter $p$ assuming values close to the critical value $p_c$, the cluster numbers scale as

$$n_s(p) = s^{-\tau} f[(p - p_c)s^{\sigma}] \qquad \text{(for } p \approx p_c\text{)}, \quad (2)$$

where $s$ is the size of a cluster. The scaling function $f$ has the property $f(0) = 1$ and accounts for the fact that a power law dependence is correct only in the case of $p = p_c$.

Implicitly introduced by Eq. (2) are two critical exponents of percolation theory: $\sigma$ and $\tau$. With the definition $s_\xi = (p - p_c)^{-1/\sigma}$, we can rewrite Eq. (2) as

$$n_s(p) = s^{-\tau} f\left[\left(\frac{s}{s_\xi}\right)^{\sigma}\right]. \quad (3)$$

This leads to the interpretation of $s_\xi$ as a crossover size for the cluster sizes from power law abundance for $s \ll s_\xi$ to exponentially rare clusters of size $s \gg s_\xi$.

A special case of the general Eq. (2) is, for example, the scaling implied by the Fisher droplet model [13],

$$\langle n_Z \rangle = \left\langle \frac{N_Z}{Z_0} \right\rangle = q_0 Z^{-\tau} \exp\left[ \frac{Z\Delta\mu}{T} - \frac{c_0 \epsilon Z^{\sigma}}{T} \right], \quad (4)$$

where $Z$ is the size of a droplet and $\epsilon = (T_c - T)/T$ is the scaled control parameter. From this equation we expect a straight line when plotting $\langle n_Z \rangle / q_0 Z^{-\tau}$ in a semilog plot (compare Fig. 2) vs $\epsilon Z^{\sigma}$ in the vicinity of the critical point, provided the scaling behavior holds. In addition, the straight line should have the property of $f(0) = 1$. (Here it is assumed that the bulk factor $\exp[Z\Delta\mu/T]$ is close to unity, an assumption that is supported by earlier findings of Elliott *et al.* [14].)

In the context of the percolation model, the same scaling behavior can be expected if one substitutes the temperature $T$ by the bond breaking probability $p_b$. Again, the cutoff function $f$ in the scaling equation is then given by the exponential factor in Eq. (4). Thus, one can find numerical values for $\sigma$, $\tau$ and $T_c$, or $p_c$, respectively, by conducting a $\chi^2$ optimization procedure for the parameter set for which the log of the scaled yield, $\langle n_Z \rangle / q_0 Z^{-\tau}$, as a function of the scaled control parameter, $\epsilon Z^{\sigma}$, collapses on a single straight line best fit.

The result of this optimization procedure for the unfiltered model calculation is shown in Fig. 2. The values of the critical parameters extracted are $\sigma = 0.5 \pm 0.1$, $\tau = 2.18 \pm 0.01$, in good agreement with the accepted values of standard 3D percolation on infinite lattices, $\tau = 2.18$, and $\sigma = 0.45$. We also find $p_c = 0.65$. This shows that $p_c$, unlike $\tau$ and $\sigma$, is strongly affected by finite-size scaling corrections, in accordance with the findings of [4,15].

Having shown that the method yields reasonable results in a known case, we apply it to the determination of the critical parameters of the ISiS data. In previous analyses
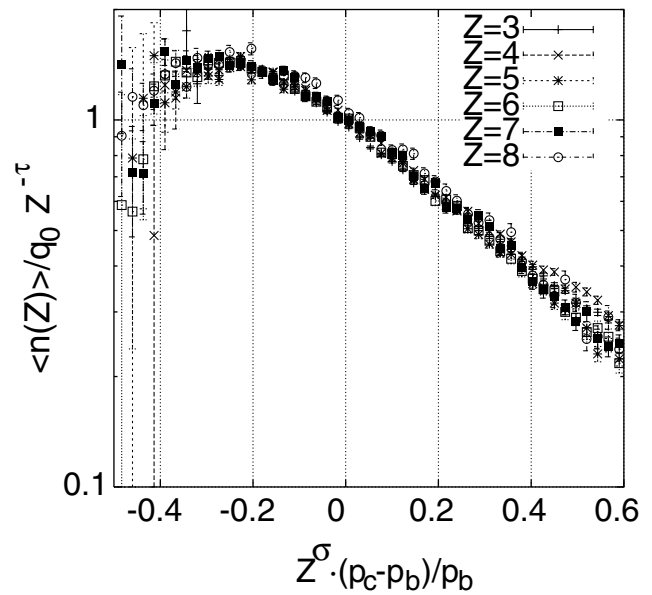


FIG. 2.   Scaled fragment yields as a function of the scaled control parameter for the model calculations. The yields for the $Z = 3$, 4, 5, 6, 7, and 8 fragments are shown.

of this kind, no corrections for sequential decays, feeding, population of particle unstable resonances, and all other final state modifications of the charge yield spectrum were considered (see [16]). We have paid particular attention to these effects in the work presented here.

To estimate the corrections for sequential decays, we start with our model calculations. They can reproduce almost all features of the data and in particular the charge yield spectrum, after detector and final state interaction corrections. Since we know the model yields before and after the corrections, we can extract the charge resolved correction factors. These factors are then applied to the experimental data. The result of the resulting $\chi^2$ optimization procedure is shown in the left hand side of Fig. 3. The values of the critical parameters obtained are $\sigma = 0.5 \pm 0.1$, $\tau = 2.35 \pm 0.05$, and $T_c = 8.3 \pm 0.2$ MeV. The contours of the $(\sigma, \tau) - \chi^2$ fit are shown in Fig. 4 for $T_c = 8.3$ MeV.

If one neglects the corrections for detector acceptance and sequential decays, then there is no way that the yields for different light fragments can be collapsed onto a single scaling graph. On the right hand side of Fig. 3 we show the best fit result of the $\chi^2$ optimization for that case. It is obvious that the collapse is not achieved. This comparison can also be made for $Z > 6$. The ISiS data set has elementally resolved yields for $Z < 17$. But the effects of the corrections are strongest for the lightest element.

To summarize, a three-step percolation model for nuclear multifragmentation reactions has been introduced. In order to reduce unnecessary model dependences we have chosen to utilize the information on source size and excitation energy deposition provided in the experiment. For the fragmentation part of the model we use the well-known percolation approach. We find that our calculations are
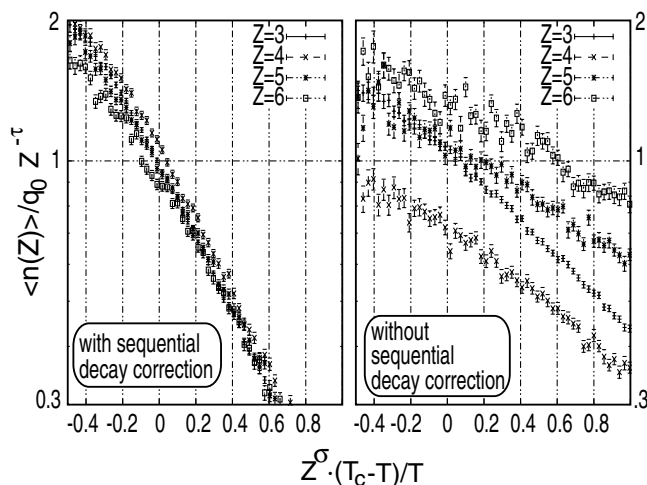
FIG. 3.  Scaled fragment yields as a function of the scaled control parameter for $Z = 3$, 4, 5, and 6. The left hand side shows the results of the correct inclusion of secondary decay corrections, and the right hand side shows the best fit possible when omitting these corrections.

in very good agreement with the data. Since the infinite size limit of the model contains a second order continuous phase transition for a certain range of excitation energies that is covered by a subset of the events in the present data set, we interpret this agreement as strong circumstantial evidence for a continuous phase transition in nuclear matter. This interpretation is supported by a scaling analysis. We find that the data show very strong scaling behav-
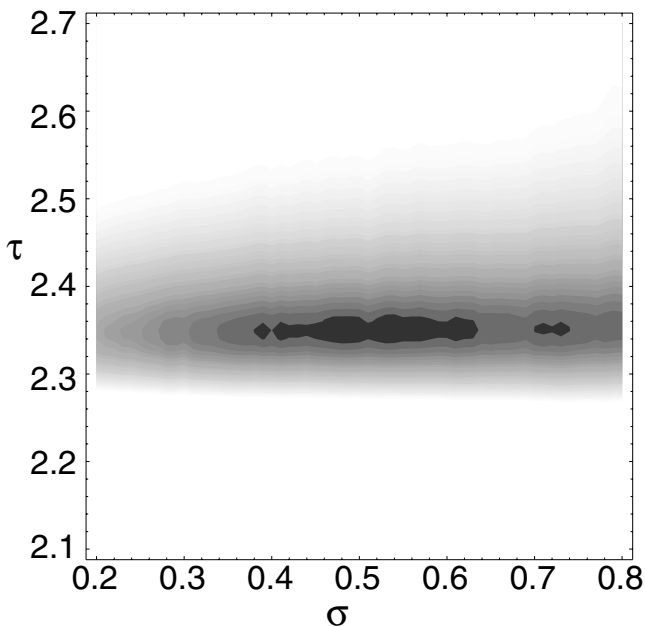
ior, as expected in the vicinity of the critical point. The critical parameters extracted from a $\chi^2$ optimization procedure have the values $\sigma = 0.5 \pm 0.1$, $\tau = 2.35 \pm 0.05$, and $T_c = 8.3 \pm 0.2$ MeV.

*Corresponding author.
  Email address: bauer@pa.msu.edu
†Current address: Département de physique, génie physique et optique, Unversité Laval, Ste-Foy, Québec, Canada G1K 7P4.
‡Current address: Physics Division P-23, Los Alamos National Laboratory, Los Alamos, NM 87545.
§Current address: LPC de Caen, 14050 Caen cedex, France.
‖Current address: Rush Presbyterian, St. Luke Medical Center, Chicago, IL 60612.

[1] W.-C. Hsi *et al.,* Phys. Rev. Lett. **79**, 817 (1997); L. Beaulieu *et al.,* Phys. Lett. **163B**, 159 (1999); L. Beaulieu *et al.,* Phys. Rev. C **63**, 031302 (2001).
[2] K. Kwiatkowski *et al.,* Phys. Lett. B **423**, 21 (1998); J. P. Bondorf, A. S. Botvina, A. S. Iljinov, I. N. Mishustin, and K. Sneppen, Phys. Rep. **257**, 133 (1995); T. Lefort *et al.,* Phys. Rev. C **62**, 031604(R) (2000); D. Durand, Nucl. Phys. **A541**, 266 (1992); W. Friedman, Phys. Rev. C **42**, 667 (1990).
[3] J. A. Hauger *et al.,* Phys. Rev. C **62**, 024616 (2000).
[4] W. Bauer *et al.,* Phys. Lett. **150B**, 53 (1985); Nucl. Phys. **A452**, 699 (1986); W. Bauer, Phys. Rev. C **38**, 1297 (1988).
[5] X. Campi, J. Phys. A **19**, L917 (1986); T. Biro *et al.,* Nucl. Phys. **A459**, 692 (1986); J. Nemeth *et al.,* Z. Phys. A **325**, 347 (1986); L. Phair *et al.,* Phys. Lett. B **314**, 271 (1993); Y. M. Zheng, J. Richert, and P. Wagner, J. Phys. G **22**, 505 (1996); G. Kortemeyer *et al.,* Phys. Rev. C **55**, 2730 (1997).
[6] T. Li *et al.,* Phys. Rev. Lett. **70**, 1924 (1993); T. Li *et al.,* Phys. Rev. C **49**, 1630 (1994); see also A. Coniglio and W. Klein, J. Phys. A **13**, 2275 (1980); X. Campi and H. Krivine, Nucl. Phys. **A620**, 46 (1997).
[7] J. B. Elliott *et al.,* Phys. Lett. B **381**, 35 (1996); M. L. Gilkes *et al.,* Phys. Rev. Lett. **73**, 1590 (1994).
[8] G. Wang *et al.,* Phys. Rev. C **53**, 1811 (1996).
[9] S. Pratt, W. Bauer, Ch. Morling, and P. Underhill, Phys. Rev. C **63**, 034608 (2001); W. Bauer, S. Pratt, Ch. Morling, and P. Underhill, Heavy Ion Phys. **14**, 29 (2001).
[10] W. Bauer and A. Botvina, Phys. Rev. C **52**, R1760 (1995); **55**, 546 (1997).
[11] W. Bauer and W. A. Friedman, Phys. Rev. Lett. **75**, 767 (1995).
[12] M. Kleine Berkenbusch, M.S. thesis, Michigan State University, 2001.
[13] M. E. Fisher, Physics **3**, 255 (1967).
[14] J. B. Elliott *et al.,* Phys. Rev. Lett. **85**, 1194 (2000).
[15] H. M. Harreis and W. Bauer, Phys. Rev. B **62**, 8719 (2000).
[16] J. B. Elliott *et al.,* eprint nucl-ex/0104013 (2001).

FIG. 4.  $\chi^2$ optimization contours for the corrected ISiS data. A value of $T_c = 8.3$ MeV was used.